Experimental Characterization of Mobile Fading Channels Aiming the Design of Non-Wearable Fall Detection Radio Systems at 5.9 GHz

Farhad Firoozi, Alireza Borhani, and Matthias Pätzold

Faculty of Engineering and Science, University of Agder P.O. Box 509, 4898 Grimstad, Norway

Emails: {farhaf14, alireza.borhani, matthias.paetzold}@uia.no

Abstract—One of the major concerns for the independent living of elderlies is a fall incident. To decrease human interaction errors and user privacy concerns of existing fall detection systems, a new generation of fall detection systems is emerging. The new trend is to design non-wearable devices that can monitor the physical activities of the home user using radio waves reflected off the body. This paper reports an in-home radio measurement campaign at 5.9 GHz, which has been conducted to study the impacts of different physical activities of the user, including fall incidents, on the channel transfer function (CTF) and the power delay profile (PDP) of indoor mobile radio channels. The home is equipped with a radio channel sounder that records the impulse response of the channel, in which the user behaves like a moving scatterer. Experimental results reveal that fingerprints of the user activities on the time-variant (TV) CTF and the TVPDP can be traced and classified both illustratively and computationally. It is shown that a so-called differential PDP (DPDP) ignores fine variations of the channel and highlights major changes, such as a fall incident. Mathematical expressions for the key characteristics of the channel are also derived under non-stationary propagation conditions. The results in this paper are important for the development of robust detection algorithms, which are an integral part of emerging fall detection systems using radio waves.

I. INTRODUCTION

According to the 2015 Aging Report [1] released by the European Commission, more than 30 % of the Europeans will be over 65 by 2060. This will create a crucial demand for in-home eldercare, specially for those who live alone. One of the major challenges within eldercare is the detection of fall incidents. Such incidents may result in serious physical and psychological consequences [2]. Detecting falls successfully leads to immediate assistance and reduces negative impairments to health. Triggered by the aforementioned demand, there is a new trend in developing indoor solutions for monitoring elderlies living independently at home.

Existing systems for detecting indoor incidents are categorized into two major classes [3]. The first class includes wearable systems, such as smartphones, bracelets, necklaces, and belts (e.g., Lifeline by Philips [4] and Angel4 by SENSE4CARE [5]) equipped with diverse sensors; and the second class comprises context-aware systems, such as vision sensors, video cameras, and smart floors (e.g., the floor sensor system in [6]), which will be placed in designated indoor areas. The wearable systems arise several user-end concerns, such as user privacy, user acceptance, and user training. For instance, a user may simply forget to wear the device or may feel uncomfortable carrying an extra system. The context-aware systems cover regularly a limited region and are limited to the places where the sensors have been previously deployed [7].

To overcome the aforementioned drawbacks, a new generation of context-aware systems is emerging. The new trend is to design a wireless (non-wearable) radio communication system that is able to monitor the user activity by analyzing radio waves reflected off the body without any user involvement in the system functionality. This fall detection method is a research-level approach that is not mature yet and has not resulted in any actual product in the market so far.

In this context, a number of systems have been proposed by a research group at Massachusetts Institute of Technology (MIT). WiZ [8] and WiTrack [9] are examples of non-wearable tracking/gesture recognition systems that are designed according to the principles of radar systems. Given a frequency-modulated carrier wave (FMCW) radar operating between the 5.56 GHz and 7.25 GHz bands, the time-of-flight (TOF) of radio waves is measured. The device estimates the TOF of the signal traveling from the transmitting antenna to the reflecting object and to each of the receiving antennas. Owing to the position of the antennas, the system is able to detect the position of the target. Several research studies propose different fall detection systems based on channel state information (CSI) and received signal strength (RSS) of the radio channel. In [10], the authors propose a non-wearable indoor fall detection system, called WiFall. This system has been implemented and evaluated on two laptops equipped with an Intel WiFi link 5300 wireless network interface controllers (NICs) operating on the IEEE 802.11n standard and two access points (APs). All the NICs and APs have been equipped with three antennas operating in the 5 GHz band. The task of NICs is to collect the CSI. In [11], the authors develop a fall detection system using array antennas. This system exploits the reflected radio waves from the objects to detect the activities of the person by observing the changes in the RSS. Employing a set of RF sensor nodes for detecting the spatial position of a person was proposed in [12]. Therein, the variations of the RSS is the chosen detection metric.

However, other radio channel characteristics, such as the average duration of fade, level-crossing rate, Doppler power spectral density (PSD), channel transfer function (CTF), and the power delay profile (PDP) are also affected by the physical

activities of the user in the propagation area. These properties may be more beneficial for the development of robust incident detection algorithms, and subsequently for the design of non-wearable incident detection radio systems of high reliability. Given an indoor propagation area with the presence of moving scatterers (users), the non-stationary channel characteristics are difficult to model and to analyze.

This paper carries out an empirical proof-of-concept to verify that fingerprints of user activities can be observed and detected in the CTF and PDP of indoor radio channels. To this aim, we conduct an indoor radio measurement campaign at 5.9 GHz to record the time-variant CTF (TVCTF) affected by a moving person, who acts out the following three scenarios: a walking, a falling, and a sitting scenario. The chosen operating frequency falls into the sub-6 GHz frequency band, which is of great interest for the development of 5G systems (healthcare verticals). We derive the time-variant channel impulse response (TVCIR) and time-variant PDP (TVPDP) from the TVCTF. A subtractive function, called differential PDP (DPDP), is then defined and used to study the variations of the non-stationary channel characteristics affected by physical activities of the person in the living area. Mathematical expressions are also derived for the main characteristic properties under non-stationary conditions. The results demonstrate that the human activities are recognizable and distinguishable through the temporal variations of the CTF and PDP. It is also shown that the channel is frequency selective and non-stationary.

The remainder of this paper is organized as follows. Section II describes the measurement methodology and the corresponding scenarios. The channel characteristics of interest are presented in Section III. In Section IV, the empirical results collected from the measurement campaign are presented and discussed. Finally, the paper is concluded in Section V.

II. MEASUREMENT SETUP AND SCENARIOS

A. Setup

The measurement campaign was conducted using a radio channel sounder developed at the Norwegian University of Science and Technology (NTNU) and owned by Super Radio AS. The operating frequency of the channel sounder is 5.9 GHz. The signal bandwidth is 100 MHz, which—according to Nyquist's sampling theorem—allows for a sampling frequency f_s of 200 MHz. The transmitter (Tx) has been configured to transmit 833 chirps per second, while each chirp contains 2560 samples. The transmit power has been set to +17 dBm.

Fig. 1 shows parts of the propagation area, the Tx and receiver (Rx) systems, and the location of the Tx and Rx antennas. The measurements have been conducted in a living room of a typical Norwegian house located in Grimstad, Norway (see Fig. 1). The living room has standard furniture, such as a sofa, table, bookshelf, fireplace, etc. The walls and the floor of the building are wooden. The room area is 35.91 m². A schematic plot of the measurement setup/environment is shown in Fig. 2. The figure also displays the approximate trajectory of the user towards the potential terminating points, which are chosen according to the considered scenario (see Section II-B).

The Tx and Rx are equipped with single omnidirectional antennas. The height of the Tx (Rx) antenna is 1.6 m (0.6 m) and the antenna elevation angle is 20° (0°) with respect to the floor. Before the measurements have been carried out, the Tx and Rx were synchronized using a global positioning system (GPS) clock. The CTF has been recorded and processed in a laptop equipped with an Intel 2.4 GHz Core i5 central processing unit and a Ubuntu 14.04 operating system. According to Fig. 2, the Tx has a line-of-sight (LOS) to the Rx. The distance between Tx and Rx is 6.5 m. The dashed lines demonstrate the scattered signals by the moving or fixed scatterers. The only moving scatterer is the user. There exist several fixed scatterers in the environment, but the figure shows only the bookshelf and the table as two examples.
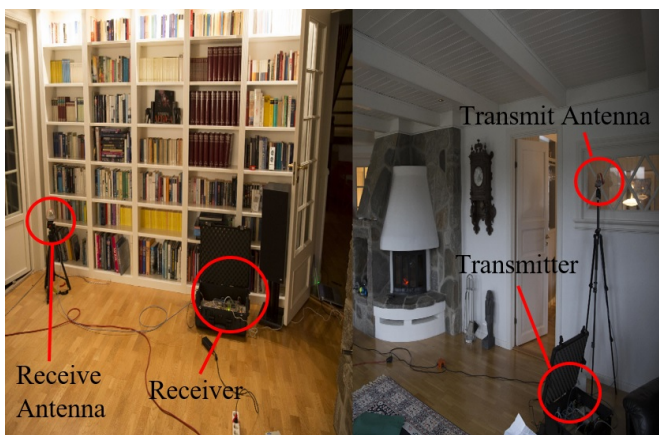

Fig. 1: Parts of the living area, where the measurement campaign has been conducted.
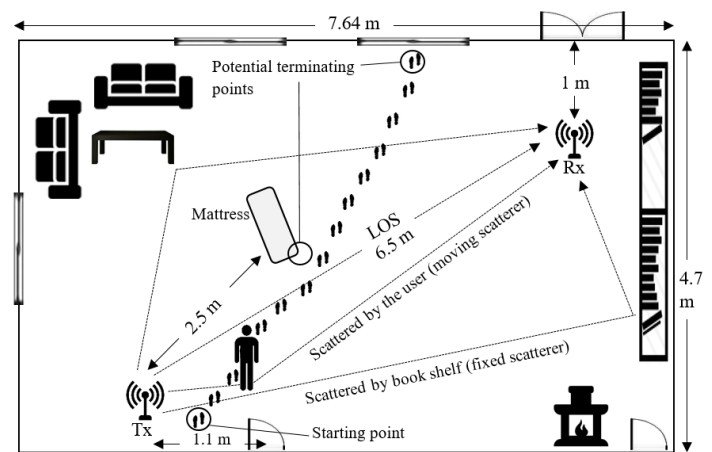

Fig. 2: A schematic presentation of the propagation environment, illustrating both fixed scatterers and a single moving scatterer (user).

B. Scenarios

A 30-year-old man[1] (with 1.78 m height) has been asked to walk along the trajectory shown by the footprints in Fig. 2. He has been asked to perform the following scenarios with a relatively slow speed similar to elderlies.

- *Reference*: The user is not in the room, and there is no physical activity in the living area. This scenario has been designed to compare the characteristics of a stationary radio channel with the non-stationary ones determined by the next three scenarios.
- *Walking*: The user walks with a relatively slow speed along the illustrated trajectory (see Fig. 2) towards the window. This scenario has been designed to analyze the impact of walking as a typical daily activity on the channel characteristics.
- *Falling*: The user walks with a relatively slow speed along the illustrated trajectory in Fig. 2 up to the mattress and then performs a relatively sharp fall. This scenario has been designed to study the impact of rapid movement variations of the user on the characteristics of the radio channel.
- *Sitting in a chair*: The user walks slowly along the illustrated trajectory and then sits down in a wooden chair at the same place where the mattress was located (see Fig. 2). This scenario has been designed to study the variations of the channel characteristics in case of sitting in a chair. This scenario and its results should be distinguishable from that in case of falling on a mattress at the same location.

III. COMPUTING OF THE MEASURED PDP

The idea of a non-wearable fall detection radio system is based on the hypothesis that activity features of moving persons affect the radio channel characteristics. Although, the spectral characteristics, such as the Doppler PSD, may provide a good insight into the temporal variations of the channel (moving person), the focus of this paper is more on exploiting the temporal characteristics of the PDP. The channel sounder used in the campaign measures the CTF from which all other channel properties can be derived. This paper studies the CTF and the PDP of the channel for the scenarios discussed in Section II-B. In what follows, we explain how the measured PDP can be computed from the measured CTF. The proposed method allows us to analyze the empirical results (see Section IV) collected from the measurement campaign.

The TVCIR $h(\tau', t)$ can be computed by taking the inverse Fourier transform of the TVCTF $H(f', t)$ with respect to the frequency variable f' [13, p. 59], where τ' indicates the propagation delay and t is the time variable. The corresponding TVCIR can be expressed by

$$h(\tau', t) = \sum_{n=0}^{N} \mu_n(t)\delta(\tau' - \tau_n'(t)) \tag{1}$$

[1]The acting was performed by a 30-year-old person, as simulating the falls with an elderly would increase the risk of injuries.

, where N is the number of scatterers, $\mu_n(t)$ is a non-stationary process indicating the time-variant complex channel gain, $\delta(\cdot)$ denotes the Dirac delta function, and $\tau_n'(t)$ describes the time-variant propagation delay of the nth multipath component. The experimental setup described in Section II is a fixed-to-fixed (F2F) communication scenario in the presence of both fixed and moving scatterers. The TVCIR of the underlying F2F scenario is given by a sum of scattered components ($n = 1, 2, \ldots, N$) and a LOS component ($n = 0$). According to the measurement scenario, the LOS component is present unless it is blocked by the moving scatterer (user).

For calculating the TVPDP, we consider the expression of the TVCIR in (1). This equation is comprised of the non-stationary process $\mu_n(t)$ and the Dirac delta function $\delta(\tau' - \tau_n'(t))$. The values of the time-variant delays $\tau_n'(t)$ are known from the measurement campaign. By computing the square of the absolute value of the time-variant complex channel gain, i.e., $|\mu_n(t_k)|^2$ for $0 \leq k \leq N$, we obtain the instantaneous power of the nth propagation path. Then, the instantaneous power of the nth propagation path can be represented as $|\mu_n(t_k)|^2\delta(\tau' - \tau_n'(t_k))$. In this way, the corresponding TVPDP can be expressed as

$$S_{\tau'}(\tau', t) = \sum_{n=0}^{N} |\mu_n(t)|^2\delta(\tau' - \tau_n'(t)). \tag{2}$$

If there is no motion or slow motion in the environment, no rapid variations can be seen in the TVPDP $S_{\tau'}(\tau', t)$. This fact motivates us to introduce the DPDP which is defined as $\Delta S_{\tau'}(\tau', t) = S_{\tau'}(\tau', t + \epsilon) - S_{\tau'}(\tau', t)$, where ϵ is a properly chosen increment in time. This function removes the fine variations of the PDP and highlights rapid changes.

IV. EXPERIMENTAL RESULTS AND DISCUSSIONS

In this section, we present the empirical collected data from the conducted measurement campaign. As a guideline, we first present and discuss the results collected from the reference scenario. Then, we show how the defined physical activity in each scenario can be detected and distinguished from that of other scenarios.

To provide a quantitative insight into the illustrative results, we introduce a metric, called D-parameter, which computes the standard deviation of the DPDP over a certain period of time. First, the measurement time is equally divided into P windows. For each window, the average value of the corresponding data is calculated over delay to represent the data as a single value at each time point. Let σ_i, $1 < i \leq P$, denote the standard deviation of these values over time. Then, the D-parameter within the ith window is calculated as $D_i = \sigma_i/\Delta t_i$, where Δt_i is the number of seconds in the time window i. In what follows, we consider the measurement time $2\,s \leq t \leq 10\,s$ of the recorded data and divide it into $P = 3$ time windows to compute D_1, D_2, and D_3. The reason for choosing $P = 3$ is that the activities of the user can roughly be divided into three phases, namely walking, falling, and resting.

A. Reference Scenario

Fig. 3 illustrates the absolute value $|H(f', t)|$ of the TVCTF. It can be observed that the TVCTF is smooth and without notable variations over time, as there is no moving person in the environment. The stationarity of the TVCTF allows us to conclude that $|H(f', t)| \approx |H(f')|$.

Fig. 4 illustrates the absolute value of the DPDP $|\Delta S_{\tau'}(\tau', t)|$, by using $\epsilon = 1/5\,s$ (this value has been chosen for all scenarios). Referring to this figure, no major changes in the DPDP can be seen as time passes. This can also be supported by the values of the D-parameter. The calculated D values associated with $2\,s \leq t \leq 4\,s$, $5\,s \leq t \leq 7\,s$, and $8\,s \leq t \leq 10\,s$ are $D_1 = 0.09$, $D_2 = 0.07$, and $D_3 = 0.2$, respectively. These values reveal that the variation of the TVPDP is very slow through all the three time windows, confirming the absence/resting phase of the test person in the propagation environment.
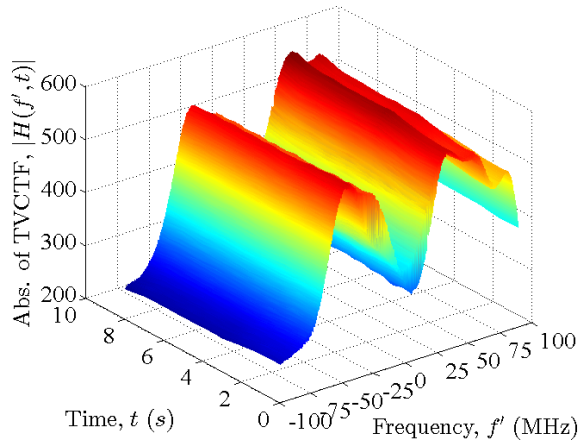
B. Walking Scenario

The absolute value of the measured TVCTF $|H(f', t)|$ associated with the walking scenario is shown in Fig. 5. In this case, the test person walks from the starting point and follows the trajectory shown in Fig. 2. It can be observed that the walking user causes major fluctuations in the TVCTF in both time and frequency. The user walks through the LOS at about the 6th second. The impact of the blocked LOS component can be observed in Fig. 5 at $t \approx 6\,s$, when the TVCTF decreases significantly. Comparing the TVCTF of this scenario with that of the reference scenario, one can verify the fingerprints of the user mobility on the TVCTF.

Fig. 6 displays the absolute value $|\Delta S_{\tau'}(\tau', t)|$ of the DPDP for the walking scenario. Referring to this figure, the DPDP fluctuates along the time axis. The highest variation occurs when the user intercepts the LOS component. These observations can also be verified by the following D-parameter values: $D_1 = 5.87$, $D_2 = 13.05$, and $D_3 = 6.27$. Note that D_2 (associated with $5\,s \leq t \leq 7\,s$) is almost twice of its neighboring D values and almost 186 times of D_2 in the ref-

Fig. 3: The absolute value of the TVCTF $|H(f', t)|$ associated with the reference scenario.

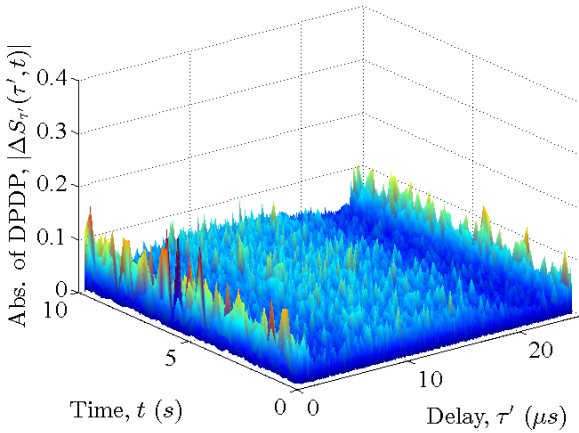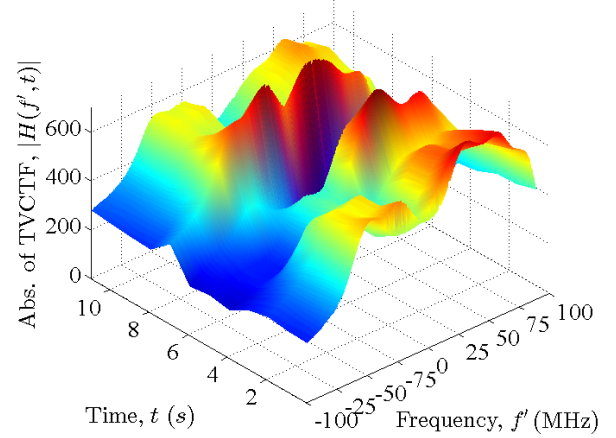Fig. 5: The absolute value of the TVCTF $|H(f', t)|$ associated with the walking scenario.

Fig. 4: The absolute value of the DPDP $|\Delta S_{\tau'}(\tau', t)|$ associated with the reference scenario.
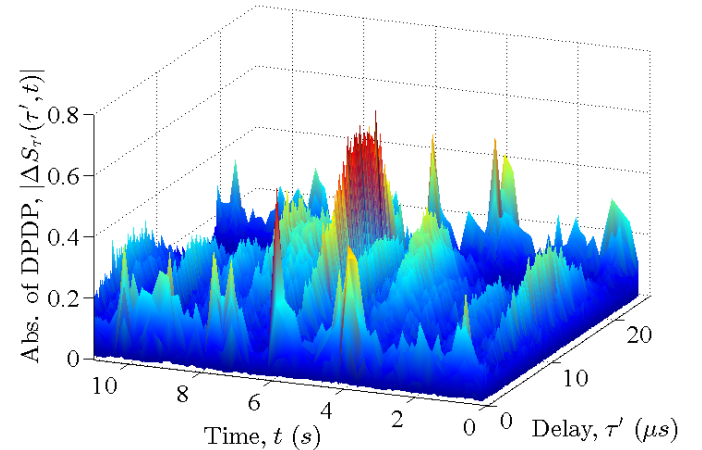

Fig. 6: The absolute value of the DPDP $|\Delta S_{\tau'}(\tau', t)|$ associated with the walking scenario.

erence scenario. Regarding the first time window, $D_1 = 5.87$ is around 65 times larger than that of the reference scenario. This considerable increase of the D-parameter demonstrates the non-stationarity of the channel due to the presence of a mobile scatterer (walking user).

C. Falling Scenario

Fig. 7 demonstrates the absolute value of the TVCTF $|H(f', t)|$ associated with the falling scenario. In this scenario, the user walks on the path and simulates a fall incident at about the 6th second according to the used chronometer. Note that the falling incident is simulated at the same time that user blocks the LOS. This can also be confirmed in Fig. 7, where $|H(f', t)|$ decreases significantly at $t \approx 6$ s. This drop is more severe and may be distinguished from the drop showed in the walking scenario. After the fall incident, $|H(f', t)|$ enters a stable phase, which is similar to the results of the reference scenario. The stable phase is counted as lying motionless on the floor after the incident.

Fig. 8 exhibits the absolute value $|\Delta S_{\tau'}(\tau', t)|$ of the DPDP for the falling scenario. The DPDP fluctuations can
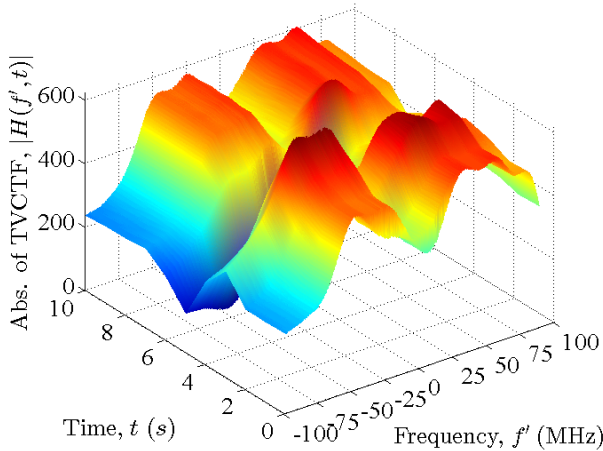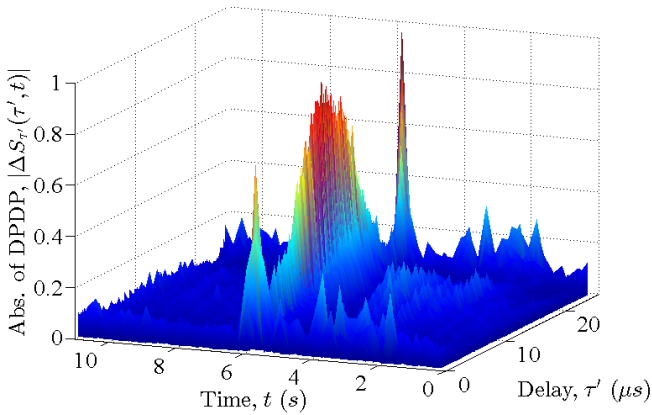
be observed during the walking period, i.e., $2\,s \le t \le 4\,s$. The variations increase considerably when the user falls down at about $t = 6$ s. Thereafter, the channel is more stable as the user is lying on the floor without any significant movement. If we divide the plot into three major parts along the time axis, namely before, during, and after the incident, it can be observed that the first part is highly similar to that of the walking scenario. The third part follows almost the same pattern as the reference scenario. The only unique and discernible behavior occurs in the second part, within which the fall incident happens. These variations can be verified by the values of the D-parameter. The calculated value for the first time period is $D_1 = 4.66$, which is comparable with $D_1 = 5.87$ in the walking scenario. Owing to the fall incident, the value of D_2 increases to 21.42, which is almost 5 times of D_1 in the same scenario and 1.6 times of that in the walking scenario. In the last time window, i.e., $8\,s \le t \le 10\,s$, one obtains $D_3 = 0.2$, which is close to that of the reference scenario, indicating that the user does not move after the fall.

D. Sitting in a Chair Scenario

Fig. 9 demonstrates the absolute value $|H(f', t)|$ of the TVCTF for the sitting scenario. As the user walks, $2\,s \le t \le 4\,s$, the TVCTF changes in both time and frequency. During sitting down in the chair, much higher variations can be observed in the TVCTF $|H(f', t)|$. When the user is sitting, the TVCTF is more stable, but there are still some relatively slow variations, which are different from those of the walking and falling scenarios at the same time window.

Fig. 10 illustrates the absolute value $|\Delta S_{\tau'}(\tau', t)|$ of the DPDP associated with the sitting scenario. Referring to this figure, the DPDP fluctuates almost along the whole time axis. The fastest variations occur when the user sits in the chair. These observations can also be validated by the following D-parameters: $D_1 = 5.94$, $D_2 = 8.69$, and $D_3 = 1.08$. During the first period, the variations are similar to the walking scenario. Since the user sits in the chair with a relatively low

Fig. 7: The absolute value of the TVCTF $|H(f', t)|$ associated with the falling scenario.

Fig. 8: The absolute value of the DPDP $|\Delta S_{\tau'}(\tau', t)|$ associated with the falling scenario.
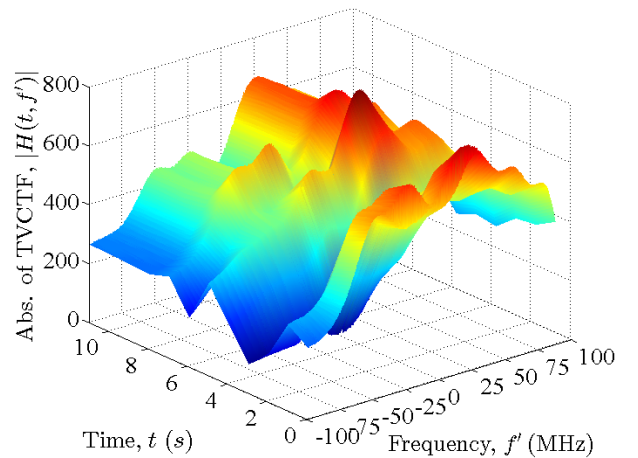

Fig. 9: The absolute value of the TVCTF $|H(f', t)|$ associated with the sitting scenario.
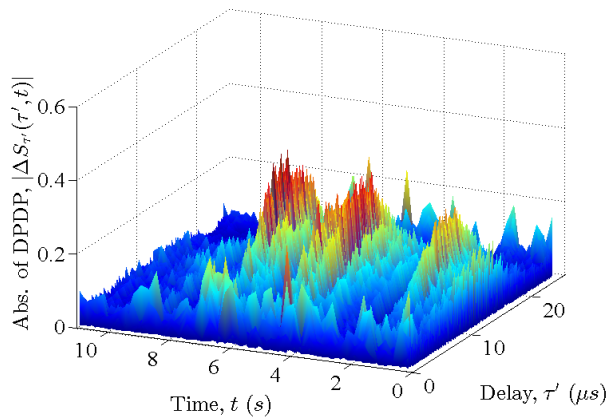
Fig. 10: The absolute value of the DPDP $|\Delta S_{\tau'}(\tau', t)|$ associated with the sitting scenario.

speed, the value of $D_2 = 8.69$ is lower than those in the walking ($D_2 = 13.05$) and falling ($D_2 = 21.42$) scenarios. Moreover, the value of $D_3 = 1.08$ in this scenario is less than that of the walking scenario ($D_3 = 6.27$) and higher than that of the falling/reference ($D_3 = 0.2$) scenario. This indicates that the user is neither highly active nor completely motionless. The user sits already in the chair and may have minor body motions.

V. CONCLUSIONS

This paper has reported an indoor radio measurement campaign at 5.9 GHz, which was designed to study the impacts of the user mobility (as a moving scatterer) on the characteristics of the radio channel. It has been shown that the fingerprints of the user activities, including walking, sitting, falling, and resting, on both the TVCTF and the TVPDP can be traced and distinguished. The experimental results revealed the importance of the DPDP as a key channel property which smoothes the slow variations of the channel, while exaggerating the fast variations. It can be concluded that the D-parameter is a robust metric for the design of reliable detection algorithms.

Investigating the impacts of user activities on other channel characteristics, such as the level-crossing rate, the average duration of fades, and the Doppler PSD, is an important topic for future studies. Designing robust detection algorithms based on the channel characteristics studied in this paper is an upcoming topic of interest as well. The measurement campaign can be repeated in the presence of two or more home occupants, as well as pets, to explore if the activities are still distinguishable.

REFERENCES

[1] The European Commission, "The 2015 ageing report: underlying assumptions and projection methodologies," *European Economy*, Aug. 2014. DOI: 10.2765/76255
[2] C. J. L. Murray and A. D. Lopez, "Global and regional descriptive epidemiology of disability: Incidence, prevalence, health expectancies and years lived with disability," in *Global Burden Disease*, vol. 1, pp. 201–246, Aug. 1996.
[3] R. Igual, C. Medrano, and I. Plaza, "Challenges, issues and trends in fall detection systems," in *BioMedical Engineering OnLine*, vol. 12, no. 1, pp. 1–24, 2013.
[4] Lifeline, https://www.lifeline.philips.com/safety-solutions.html.
[5] Angel4, http://www.sense4care.com/en/products/angel4-whiteblack.
[6] H. Rimminen, J. Lindström, M. Linnavuo and R. Sepponen, "Detection of falls among the elderly by a floor sensor using the electric near field," *IEEE Trans. Information Technology in Biomedicine*, vol. 14, no. 6, pp. 1475–1476, Nov. 2010.
[7] C. Rougier, J. Meunier, A. St-Arnaud, and J. Rousseau, "Robust video surveillance for fall detection based on human shape deformation," in *IEEE Trans. Circuits and Systems for Video Technology*, vol. 21, no. 5, pp. 611–622, May 2011.
[8] F. Adib, Z. Kabelac, and D. Katabi, "Multi-person motion tracking via RF body reflections, Computer Science and Artificial Intelligence Laboratory, Tech. Rep. MIT-CSAIL-TR-2014-008, Apr. 2014.
[9] F. Adib, Z. Kabelac, D. Katabi, and R. C. Miller, "3D tracking via body radio reflections, in *Proc. 11th USENIX Conf. on Networked Systems Design and Implementation*, pp. 317–329, 2014.
[10] C. Han, K. Wu, Y. Wang, and L. M. Ni, "WiFall: Device-free fall detection by wireless networks," in *Proc. IEEE INFOCOM*, pp. 271–279, 2014.
[11] Y. Hino, J. Hong, and T. Ohtsuki, "Detecting unexpected fall using array antenna," in *Proc. IEEE PIMRC*, pp. 2104–2108, 2014.
[12] B. Mager, N. Patwari, and M. Bocca, "Fall detection using RF sensor networks," in *Proc. IEEE PIMRC*, pp. 3472–3476, 2013.
[13] M. Pätzold, *Mobile Radio Channels*, 2nd ed. Chichester, U.K.: Wiley, 2011.